

# Aluminium Foaming Monitored by Far-Infrared Thermography: Temperature Gradients and Bubble Rupture

**E. SOLÓRZANO**

**M.A. RODRIGUEZ-PEREZ**

*CellMat Group, Condensed Matter Physics Dep.  
Science Faculty, University of Valladolid  
Prado de la Magdalena S/N  
47011 Valladolid, Spain*

**F. GARCÍA-MORENO**

**N. BABCSÁN**

**J. BANHART**

*Department of Materials Science (SF3)  
Hahn-Meitner-Institut Berlin  
Glienicke Straße 100  
14109 Berlin, Germany*

## ABSTRACT

Infrared (IR) thermography was applied as a contactless method to measure the temperature distribution of metal foams in their liquid state under different heating conditions, involving high and low temperature gradients. Preliminary tests revealed the difficulty for a reliable global temperature measurement by using thermocouples.

The changing emissivity of the foaming metal's surface caused by progressive oxidation at high temperatures makes it difficult to obtain accurate temperature measurements by IR thermography. Screening the foam with a thin sheet of very low heat capacity – e.g. stainless steel foil – was found to solve this problem. Reliable temperature profiles were obtained in this way under the two different heating conditions. Significant correlations between the temperature profiles and the bubble rupture rate obtained by X-ray radiography were found.

## INTRODUCTION

Metal foams are potential materials for many applications, especially when considering not only single properties but also the unique combination of them [1]. On the other hand, many foaming routes have not yet reached the optimum development and for this reason some possible applications have not been put into reality.

In the powder metallurgical (PM) route one of the phenomena that produces inhomogeneous pore structures is the strong temperature dependence of gas release from the blowing agent, usually  $H_2$  from  $TiH_2$ , leading to early pore foaming in the hottest parts of the expanding foam. Additionally, the temperature also has an effect on the properties such as the viscosity of the metal, giving rise to

different coarsening rates for the different temperatures reached in the sample.

Some practical problems are associated to knowing the exact temperature of a foaming sample. The thermal contact between sample and thermocouples is limited to a very small and probably not sufficiently representative volume. Moreover, foaming is a dynamic process in which the sample is changing its volume and surface, so that the contact might not be good all through the foaming process, yielding an imprecise temperature in this case.

To measure the temperature distribution with good spatial resolution and without disturbing the foaming it is necessary to use a contactless method. No-contact infrared (IR) methods for measuring temperatures are interesting to be applied to the study of metal foaming. An additional advantage can be obtained if a 2D matrix detector is used. This is named *infrared thermography*, since the detector output is a 2D image in which temperature is given as a pixel depth. Thermographic techniques have been successfully applied to monitor other processes in which the temperature is a key factor such as in polymer thermoforming or metal casting [2,3]. To our knowledge, this is the first time thermography has been applied to monitor the temperature during melting and foaming of an alloy.

The aim of this work is to determine the effect of temperature on pore coarsening in the liquid state. An infrared method for a detailed measurement of the temperature distribution is used to obtain the temperature with time and spatial resolution.

## EXPERIMENTAL

A FlirSystems far infrared camera, model Thermovision A40M, has been used to acquire the surface temperature in the molten state. This model has a  $320 \times 240$  detector. The selected operating temperature range was up to  $1500^\circ\text{C}$  and

thermographic images were acquired at 12.5 fps. In addition, thermocouples were used to experimentally calibrate the emissivity of the samples under study.

Some input parameters are needed to quantify the real temperature with sufficient accuracy. The main such parameter is the *object emissivity*, but also the object-to-camera distance, the humidity and the ambient temperature should be taken into account [4]. It is important to note that the material to be inspected by the IR camera –aluminium alloys– present a high variance in emissivity. As an example, polished aluminium exhibits a very low emissivity between 0.05 and 0.1, while oxidized or anodized aluminium has an emissivity between 0.3 and 0.95. This will considerably affect the measurements as will be explained in following sections.

Two different heating systems have been used to produce high and low temperature gradients –later denoted as homogeneous and inhomogeneous– in AlSi9 samples with 0.6 wt.% of TiH<sub>2</sub>. A resistive ceramic heater was used to heat the samples in its bottom part through a mould, trying to produce an inhomogeneous temperature distribution. On the other hand, three near-mid infrared heating lamps –located in top, left and right positions– were used to heat indirectly the sample through a mould, producing a more homogeneous heating. The infrared heating lamps do not disturb the temperature reading since they emit in a different spectral range. Both experiments were kept at a similar average temperature of 660°C.

A 30×30×28 mm stainless steel square hollow profile –3 mm wall thickness– containing the samples inside was used as mould in most of the experiments. This hollow profile could also be covered with a 25 µm thick stainless steel foil on both open sides. This flat cover, in contact with the sample inside, was spray-coated from outside with graphite to increase emissivity and to improve the temperature acquisition accuracy of the infrared camera.

The thermal images obtained were analyzed by using ImageJ [5]. A pixel depth calibration with temperature was performed. In the same way, a pixel scaling according to sample size and time gap between frames, related to acquisition frame rate, were also adjusted.

Bubble rupture was characterized by using an in-situ radioscopy system [6]. Images were acquired at 0.5 fps. The experiment started just when the foam started to develop and the foam was kept at constant temperature during 700 s. A subsequent analysis of film rupture was carried out by using a dedicated software programmed to compare subsequent radioscopic images [7]. The software parameters were adjusted such that all the events detected were real ruptures and the majority of the ruptures were actually registered. The bubble rupture statistics shown here are the sum of two different experiments carried out under the same heating conditions reaching more than 3000 cumulated ruptures in each couple of experiments.

## RESULTS AND DISCUSSION

### Direct IR Study of Foaming

First experiments have been carried out by direct IR monitoring of the foaming. As Fig.1 shows, it was not possible to obtain a reliable thermal image since the temperature differences within the foam surface were not realistic. The temperatures measured in the hot spots (1) were close to twice the temperature around the spots, while temperatures in fresh foam surfaces (2) were just a third. The reflection (3) of the bottom heating ceramic plate also contributes to distorting the real temperature in the foam's bottom part. Finally, as the emissivity of the heating plate is different from that of the foam, the temperature of this object is not determined correctly.

Part of these reported errors in the thermographic images are an effect of the varying surface roughness and curvature, changing the total energy reaching the sensor. On the other hand, probably the most important and most difficult effect to be avoided is the apparent low temperature in the unoxidized new surfaces, an effect of the varying emissivity due to the different oxidation stages of these new surfaces compared with the initial surface. Additionally, if the foam is kept at high temperature for a long time, progressive oxidation leads to an apparent unphysical temperature increase. Solving this problem would require knowledge of the emissivity evolution and its distribution during foaming which is not feasible in practice.

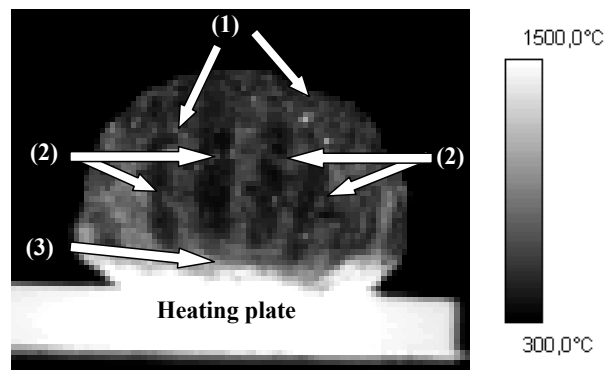


Figure 1. Thermal image of an AlSi9 sample foamed freely on a heating plate.

This problem could be solved by using a material with a very low thermal mass in permanent contact with the foam. A 25 µm stainless steel foil was used in the way reported above. As the surface of this foil is flat, temperature acquisition is accurate. Contact with the sample was assured by screwing the steel foil to the mould, and the foaming pattern was tested, obtaining a similar expansion behaviour with and without the steel screen.

### Indirect IR study of foaming

Two different foaming conditions were chosen to check the effect of the temperature distribution on foam coarsening. These will be denoted ‘homogeneous’ and ‘inhomogeneous’ in the following.

#### Homogeneous Heating

The results for homogeneous heating by using three heating lamps are shown in Fig. 2 for a time-averaged thermography of the filled mould kept at a constant temperature. Note that none of the errors previously reported appear in this case. The temperature distribution along Z in the marked rectangle is plotted in the graph.

Smoothly graded differences in temperature can be noticed from the top to the bottom of the mould. The maximum difference in temperature from bottom to top is below 25 K.

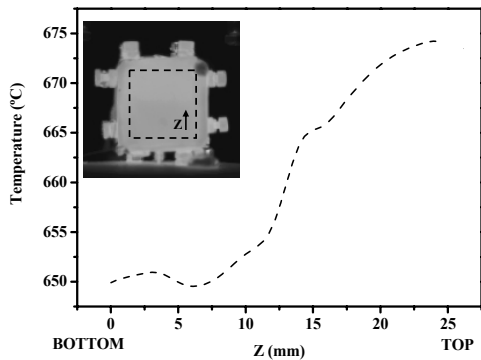


Figure 2. Thermal image and time-averaged temperature distribution along Z during homogeneous heating.

#### Inhomogeneous Heating

Inhomogeneous heating leads to a higher temperature difference from the bottom to the top in the marked rectangle as shown in Fig. 3. The pronounced temperature drop found in the top part is probably related to the missing contact between the liquid foam and the steel foil there, as the foam is vaulted in the upper part and does not touch the steel foil completely. As a consequence, the temperature in this area is much lower than expected, reaching a value below the melting point of the alloy, which obviously does not represent the true temperature of the foam. In Fig. 3, the expected temperature for the case of good contact between foam and steel foil is displayed. In this case, the temperature difference between the bottom and the top part will be close to 100 K, much higher than in the homogeneous heating condition.

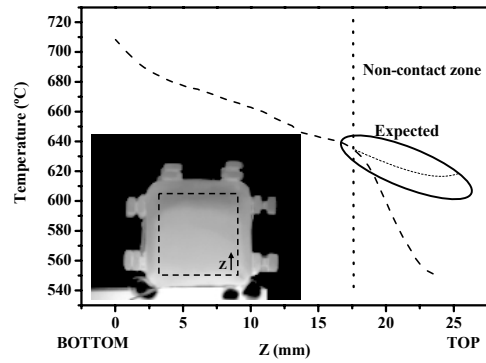


Figure 3. Thermal image and time-averaged temperature distribution along Z during inhomogeneous heating.

#### Cell wall rupture analysis

From the X-ray radioscopic analysis of cell wall ruptures in the molten state it is possible to obtain a rupture map using the coordinates of each rupture event given by the software. A 2D binning map showing the fraction of ruptures for inhomogeneous heating is presented in Fig. 4.

In the homogeneous case a higher number of ruptures are counted in the top part, where the temperature is 25 K higher compared to the bottom. These differences are not as high as in the inhomogeneous heating case, see Fig. 4b, where the fraction of cell ruptures is 4 times higher at the bottom. Drainage in the bottom part of the inhomogeneously heated mould could have played an additional role here.

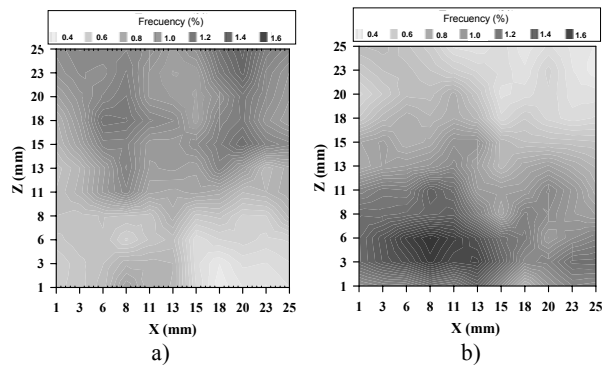


Figure 4. Map showing film rupture frequencies when foam is kept at a constant temperature during heating for 700 s.

a) homogeneous b) in-homogeneous heating.

#### Correlation with bubble rupture

As temperature and ruptures profiles present a variation in Z, but are nearly constant in X, a correlation analysis between rupture frequency and temperature was carried out. Combining the thermographic results with the computed bubble rupture obtained from the X-ray

radioscopy it is possible to prove a strong correlation, see Fig. 5.

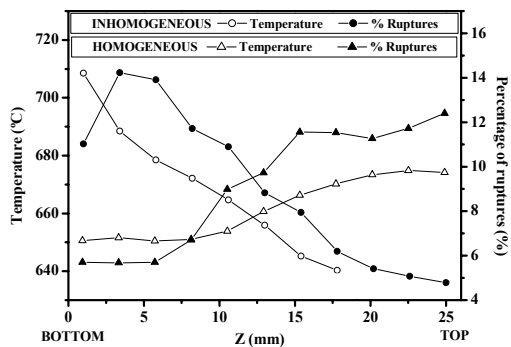


Figure 5. Film rupture and temperature gradient for homogeneous and inhomogeneous heating.

In all cases it is observed that the higher the temperature, the higher the fraction of rupture events. The inhomogeneous temperature profile was cropped since at the top it did not represent the real temperature. Moreover, at the bottom of the inhomogeneously heated sample the high temperature produced early drainage which affected bubble rupture detection by X-ray radioscopy.

## SUMMARY

A thermographic technique has been applied to study the temperature distribution during foaming of an aluminium alloy. The difficulties of directly measuring the temperature of the foam surface were evaluated. These difficulties are mainly associated to the sample roughness and the different emissivity of different areas on the surface. A screening technique inside a rectangular mould has been proposed as a suitable solution to overcome the problems reported. With this methodology, the temperature distribution under homogenous and inhomogeneous heating conditions has been characterized proving that it is possible to determine small temperature differences by this technique. The effect of the temperature gradients on bubble rupture has been studied by combining these results with X-ray radioscopy and showed significant correlations.

## OUTLOOK

It should be possible to carry out simultaneously in-situ X-ray and thermographic experiments by using special configurations based on infrared mirrors. The results obtained by such measurements would help validating finite element-based models of the temperature distribution under other much more complicated situations.

## ACKNOWLEDGEMENTS

The authors are grateful to Admatis Ltd. from Miskolc (Hungary) for their generous support with the IR camera used in this work. Funding by ESA (Projects  $\mu$ g-FOAM AO-99-075 and XRMON AO-2004-046) and financial support from the Spanish Ministry of Science to E. Solórzano for his stay in Berlin with a FPU grant (Ref-AP-2004-2908) are acknowledged.

## REFERENCES

1. Banhart, J. 2001. "Manufacture, Characterisation and Application of Cellular Metals and Metal Foams". *Progress in Materials Science* 46:559–632.
2. Bendada, A., F. Erchiqui, A. Kipping. 2005 "Understanding Heat Transfer Mechanisms During the Cooling Phase of Blow Molding using Infrared Thermography" *NDT&E International*, 38:433–441.
3. Haferkamp, H., F.-W. Bach, M. Niemeyer, R. Viets, J. Weber, M. Breuer, T. Krussel. 1999. "Tracing Thermal Process of Permanent Mould Casting". *Proceedings of the IEEE International Symposium*, 3:1442-1447.
4. ThermaCAM Researcher. User's Manual, 2004 Publ. No. 1 558 071 Rev. a74
5. Abramoff, M.D., P.J. Magelhaes, S.J. Ram, 2004 "Image Processing with ImageJ" *Biophotonics International*, 11(7):36-42.
6. García-Moreno, F., M. Fromme, J. Banhart. 2003. "Real time x-ray radioscopy on metallic foams using a compact microfocus source" *Cellular Materials*, eds. J. Banhart, N.A. Fleck, A. Mortensen, MIT-Verlag Berlin, pp. 89-93.